The effects of temperature and saltwater aging on the mode II fatigue crack growth behavior of composite-steel bonded joints

Arouche, Marcio Moreira; Egilsson, Sigurdur; Koetsier, Mathieu; Pavlovic, Marko

DOI
10.1016/j.conbuildmat.2025.143516

Publication date
2025

Document Version
Final published version

Published in
Construction and Building Materials

Construction and Building Materials 494 (2025) 143516

Contents lists available at ScienceDirect

Construction and Building Materials

journal homepage: www.elsevier.com/locate/conbuildmat

The effects of temperature and saltwater aging on the mode II fatigue crack growth behavior of composite-steel bonded joints

Marcio Moreira Arouche *, Sigurdur Egilsson, Mathieu Koetsier, Marko Pavlovic

Faculty of Civil Engineering and Geosciences, Delft University of Technology, Stevinweg 1, Delft 2628 CN, Netherlands

A R T I C L E I N F O

Keywords:
Fatigue crack growth
Environmental effects
Temperature
Aging
4-point end-notched flexure (4ENF) tests
Paris curves

A B S T R A C T

Hybrid structures built with composite and steel emerge across industries (offshore, shipbuilding, bridges, etc.) due to benefits of weight optimization, fatigue and environmental resistance. Particularly, the wrapped composite joints emerge as a new method to connect steel circular hollow sections for application in supporting structures of offshore wind turbines. The implementation of this technology requires predicting the long-term performance of the bi-material interface under operational conditions of loading and environment. This work addresses the effects of temperature and saltwater aging on the fatigue crack growth behavior of the composite-steel bonded joint under mode II loading conditions. Fatigue tests were performed using a 4-point end-notched flexure (4ENF) set up with digital image correlation (DIC). A numerically based method was applied to calculate the strain energy release rate (SERR) accounting for friction effects, geometrical and material non-linearities. The consistency of the manufacturing process was evaluated by tests performed in room conditions (21 °C). The mode II fatigue behavior of the composite-steel bonded joints remained between an upper and a lower bound of the Paris curves, characterized by composite delamination and adhesive failure, respectively. Then, the effect of temperature was assessed by experiments in −10 °C and 70 °C. Short-term temperature changes showed a significant effect on the fatigue resistance of the bonded joint, followed by changes in the failure mode. Finally, a decrease in performance was observed as a consequence of the long-term aging of specimens in saltwater for up to 549 days.

1. Introduction

Composite materials, e.g. fiber-reinforced polymers (FRPs), are increasingly popular in structural applications due to their high strength-to-weight ratio, design flexibility, and fatigue resistance. Novel designs of composite structures are introduced using FRPs in combination with traditional materials, such as steel, through adhesive bonding. These bi-material interfaces require extensive research to evaluate design, manufacturing, and operational parameters on the performance of the FRP-steel bonded structures [1,2]. In particular, composite materials are significantly influenced by environmental factors [3]. It is fundamental to predict the durability of these bi-material structures under real-life operational conditions of loading and environmental effects, such as temperature and moisture.

Several methods have studied the mechanical behavior of composite bonded joints using the fracture mechanics approach [4–6]. It assumes that a crack develops in one or a combination of three different loading modes: opening, or mode I; in-plane shear, or mode II; and out-of-plane shear, or mode III. The fracture toughness is measured as the strain energy release rate (SERR) during propagation of the crack. In the case of bonded interfaces, they present higher mechanical resistance in mode II loading conditions and is therefore the preferred loading case in the design of structures. Experimental evaluation of the mode II fracture are usually performed by end-notched flexure (ENF) tests for composite materials [7]. However, the ENF tests set-up may result in unstable crack growth when testing bonded joints. To circumvent this problem, the 4-point end-notched flexure (4ENF) tests are typically applied [8].

The performance of bonded joints can be predicted using fracture tests with cyclic loadings, or fatigue tests. Most fracture mechanics methods for evaluating fatigue resistance are based on the Paris curves, which relates the SERR to the crack growth rate during an experiment [9]. In the case of composite-steel interfaces, Weikang et al. [10] evaluated the ENF and 4ENF test methods for characterization of the interface mode II fatigue crack growth behavior. The 4ENF test set-up with displacement-controlled loadings provided a wider range of SERR measurements and lower scattering. However, analytical methods for

* Corresponding author.
E-mail address: m.moreiraarouche@tudelft.nl (M.M. Arouche).

https://doi.org/10.1016/j.conbuildmat.2025.143516
Received 8 May 2025; Received in revised form 8 July 2025; Accepted 5 September 2025
Available online 8 September 2025

calculation of the SERR based on the linear elastic fracture mechanics (LEFM) have limited application due to significant effects of geometrical nonlinearity and friction between the cracked surfaces in 4ENF tests. Moreover, crack length measurements can be obtained with the assistance of a digital image correlation (DIC) system during the tests [5,10].

Short-term changes of temperature can have a significant impact on the mechanical properties of composite materials [3]. Relevant works can be found on the effect of temperature on composite delamination. Several works [11–13] observed an increase the mode II fracture toughness of composite delamination and debonding at high temperatures together with a higher ductility, while the opposite was found in lower temperatures. Cohesive failure is usually found for room and high temperatures, while adhesive failure is common in temperatures below 0 °C because of an embrittlement of the polymer adhesive agent. Regarding composite-steel interfaces, experimental works performed by He et al. [14], using single-lap shear joints, and Ke et al. [15], using double lap joints, corelated the degradation of the bond strength with that of the tensile properties of the adhesives at high temperatures. Similar results were obtained using double strap joints [3]. Temperatures near and above the adhesive glass transition temperature (T_g) showed rapid deterioration of the joint strength and change of failure modes. Moreover, Guo et al. [16] modelled the debonding behavior of double lap shear joints at different service temperatures. These works focus on the joint strength and bond-slip behavior of the bi-material interface. Instead, the use of fracture mechanics methods to investigate effects of temperature on composite-steel bonded joints remain unexplored.

Long-term exposure to harsh environments reduces the mechanical performance of bonded interfaces [17]. Borrie et al. [18] showed the importance of protection of FRP-steel structures subjected to salt water for ensuring their strength over time. Heshmati et al. [1] observed a change from initially cohesive to interfacial failure modes accompanied by strength reductions of double-lap shear joints aged for up to three years in various environments. Exposure to thermal freeze-thaw cycles showed to cause only minor changes on the strength of the joints, while salt fog environment caused severe degradation of ultimate capacity [3]. A similar behavior was found in composite-steel bonded interfaces using peel tests after salt spray [19] and saltwater [20] aging. Additionally, a shift in failure mode is observed from thin-layer cohesive failure to adhesive failure in aged composite-steel bonded joints [21]. These works show that long-term environmental effects are critical to the ultimate strength and fracture toughness of bonded joints under quasi-static loadings. However, no relevant work addressed the combination of cyclic loadings and environmental conditions on the fatigue crack growth of composite-steel interfaces.

In the construction sector, the wrapped composite joints have been introduced as an alternative to traditional welded joints for joining steel circular hollow sections [22]. The loadings are transmitted through a wrapped glass fiber laminate with a large bonded area, promoting reduction of stress concentration, minimizing maintenance costs and increasing operational life of the structure. This innovative solution is developed for application in supporting structures for offshore wind turbines. However, the implementation of the technology requires predicting the long-term performance of the composite-steel bonded interface under combined effects of loading and environment.

In this work, the mode II fatigue crack growth behavior of composite-steel bonded joints is investigated under the effect of environmental conditions of temperature and saltwater immersion. Specimens are manufactured using the same materials and methods as indented for the wrapped composite joints. The fatigue crack growth behavior is accessed by displacement controlled 4ENF tests with DIC for crack length measurements. A numerically based model is applied to calculate the SERR accounting for geometrical non-linearities and friction effects. The consistency of the manufacturing process is evaluated by tests performed in room conditions (21 °C). Then, the effect of environmental parameters is considered in the range of operations temperatures and sea water condition. Then, tests are performed at low (-10 °C) and high (70 °C) temperatures. In addition, the long-term effect of saltwater aging is investigated after immersion for up to 549 days. Fatigue resistance is analyzed using the Paris curves and correlated to the failure mode observed in the fracture surfaces.

2. Materials and methods

2.1. Specimen manufacture

Steel-composite interface fracture specimens were manufactured using a wet lay-up process. First, steel plates S355 ($E = 210$ GPa, $\upsilon = 0.3$), with 3 mm thickness, were treated with grit blasting and degreased. Then, a primer was applied to improve the bond quality and a non-adhesive insert of 32 μm thickness was placed on the steel plate to produce a pre-cracked region. A vinyl ester resin was used as the composite matrix and adhesive agent between the composite and steel parts. Each composite ply is made of a layer of glass fiber bi-directional woven stitched to a layer of glass fiber chopped strand mat (CSM), as shown in Fig. 1. The laminated plates were allowed to cure at the room conditions of 50 ± 10 % humidity and 17 ± 1 °C. Finally, coupon specimens were cut from the plates using water jet. A scheme of the specimen geometry is shown in Fig. 2. The specimens have a nominal length of 320 mm and a nominal insert length of 90 mm. The average width (w) and thickness (H) of 25.27 ± 0.58 mm and 18.53 ± 0.73 mm, respectively, were measured from 3 different sections of each specimen using a digital caliper.

2.2. Experimental set up

The mode II fatigue behavior was accessed by the 4-point end-notched flexure (4ENF) tests. The 4ENF tests were performed in a universal testing machine coupled with a 15 kN load cell. Fig. 3 presents the ENF test scheme and test set up. The support span ($2L$) is 274 mm and the distance between the right loading and support points (L_a) is 52 mm. The steel part is always positioned on top. During the tests, a compressive force (P) is applied at the half-span of the test at the constant frequency of 4 Hz and distributed through a pin to two equally spaced load points in contact with the specimen. Specimens are loaded to 70 % the critical force in order to maintain a stable crack growth. The critical force was obtained from the first peak load before crack propagation in quasi-static tests using the same set-up [23].

Prior to the tests, a thin layer of white matt paint was coated and a random black speckle pattern was applied to the measurement surface of the specimen. A high-resolution camera (50.6 MPx) and a blue LED light source were positioned to the measurement surface to acquire the full field displacements by digital image correlation (DIC). For reference, the support points, the load points and the section of the pre-crack tip were

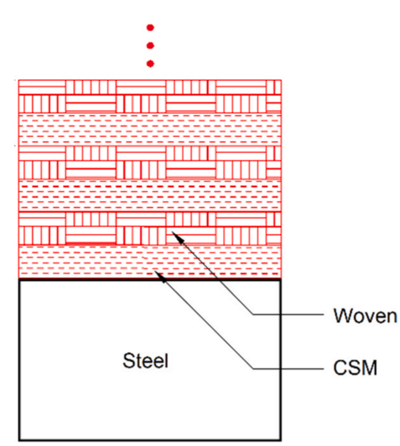

Fig. 1. Lay-up of the steel-composite bonded joints.

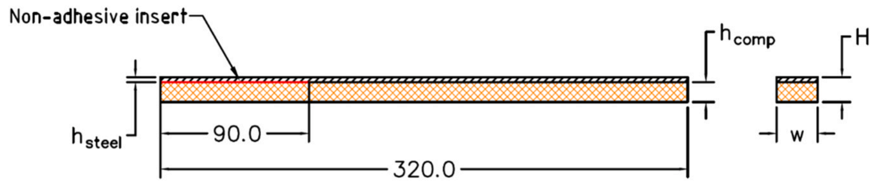

Fig. 2. Scheme of steel-composite specimen.

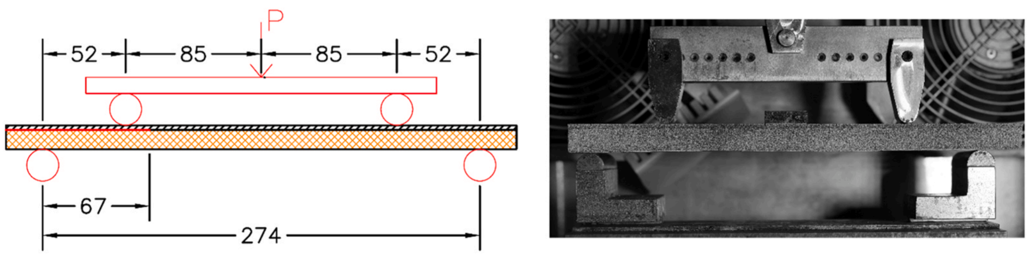

Fig. 3. 4ENF test scheme and set up (dimensions in millimeters).

marked on the measurement surface. During the tests, the controlling system takes photos at the maximum displacement after either a sequence of 500 cycles or 1 % stiffness reduction between photos (based on the machine load and displacement measurements). For image processing, surface points were recognized by a small neighborhood of a square with a side length of 19 pixels and a step size of 11 pixels set in the DIC software.

Reference tests were performed at the room temperature (RT) of 21 °C. In order to condition the specimens to different testing temperatures, a climate chamber was used in the set up for the tests at the low temperature (LT) of −10 °C and high temperature (HT) of 70 °C. Air mixing fans are placed to ensure stability of air conditions over time. Specimens were maintained in the target temperature for a minimum time of 15 h before the tests to ensure a homogeneous temperature field.

The long-term effect of moisture degradation was experimentally investigated by immersing specimens in a 500 l tank filled with 3.5 % salt mixed with demineralized water. In order to minimize the corrosion effect of corrosion on the steel part, specimens were previously coated on the steel top surface using the same resin as the composite matrix. The room temperature aging (RTA) was carried out at the constant water temperature of 23 °C. Specimens were removed from the aging tank after 222 and 549 days of immersion (RTA1 and RTA2, respectively), immediately wiped with paper tissue and tested. Table 1 shows the test matrix. A total of 5 specimens were tested in each configuration.

3. Experimental study

3.1. Crack length measurements

An experimental method is utilized to measure crack growth by analysing the shear strain on the surface of the specimens. The DIC-based method is independent of material nonlinearity and avoid the difficult visual tracking of the crack tip in mode II fracture conditions. First, an interface curve was defined along the crack path in the reference photo. Then, the shear strain is extracted from the interface curve in every photo taken during the test. The measured interface shear strains remain negligible in the bonded regions and increase due to relative movement between steel and composite arms once a crack is present, as illustrated in Fig. 4. The criterion defines the crack tip location by a threshold interface shear strain of 0.005. This value was chosen to avoid noise in the shear strain measurements from the bonded interface of the magnitude of ±0.004. This criterion is applied to obtain the crack length in every photo taken during the test.

Table 1
Test matrix.

Test series	Testing temperature (°C)	Aging time (days)	Number of tests
RT	21	-	5
LT	−10	-	5
HT	70	-	5
RTA1	21	222	5
RTA2	21	549	5

A representative measurement of the crack growth during the fatigue 4ENF tests is displayed in Fig. 5. In displacement-controlled fatigue tests, the increase of the crack length is followed by a decrease of the applied force. The curves show that the crack growth was stable from the initial stages and the crack reached a significant length of 170 mm after 30.000 cycles. This shows that the displacement values were properly defined to avoid unstable crack growth and ensure full crack development in the specimen.

3.2. Calculation of the SERR

The mode II SERR (G_{II}) of 4ENF tests can be calculated by the extended global method (EGM) [8], as follows:

$$G_{II}^{EGM} = \frac{P^2 L_a^2}{8wE_1 I_1}\left(\frac{1}{1+\psi} - \xi\right) \tag{1}$$

The parameters ψ and ξ, in Eq. (1), are the bending stiffness ratios of the arms of the specimens, given by Eqs. (2) and (3), respectively:

$$\psi = \frac{E_2 I_2}{E_1 I_1} \tag{2}$$

$$\xi = \frac{E_1 I_1}{(EI)_{eq}} \tag{3}$$

The parameters E_1 and E_2 are the flexural moduli of the upper and lower arms, respectively, I_1 and I_2 are the moments of inertia of the upper lower arms, respectively, and $(EI)_{eq}$ is the equivalent bending stiffness of the specimen.

In this study, the flexural modulus of the composite material was measured experimentally using the composite parts of each specimen separated from the steel after the fatigue tests. The flexure tests were performed with the same set up and testing conditions used for the fatigue 4ENF tests (see Fig. 3). Tests were carried out with a constant displacement of 1 mm/min. and a camera was used to take photos for DIC in a frequency of 1/3 Hz. The composite longitudinal flexure

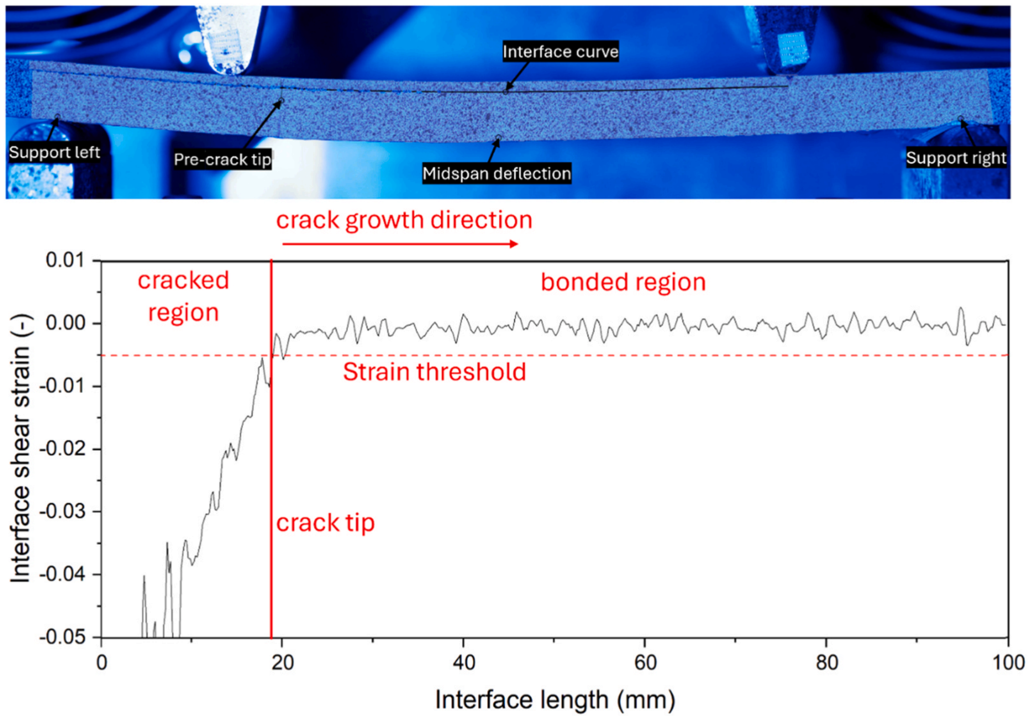

Fig. 4. Interface strain measurements with DIC.

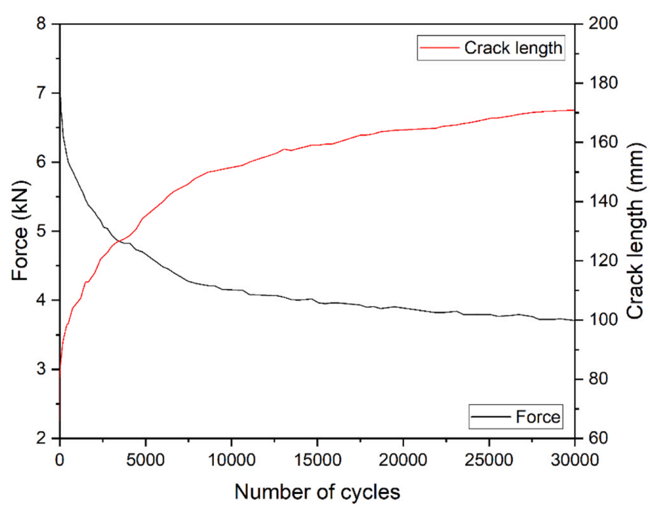

Fig. 5. Crack length measurements based on the interface strain.

modulus (E_{fx}) was calculated based on ASTM D7264 [24], using Eq. (4):

$$E_{fx} = \frac{\Delta\sigma}{\Delta\varepsilon} \tag{4}$$

Where the stress (σ) and strain (ε) are determined by:

$$\sigma = \frac{3PL}{4Bh_{comp}^2} \tag{5}$$

$$\varepsilon = \frac{48\delta h_{comp}}{11L^2} \tag{6}$$

The specimen mid-span deflection (δ) was extracted from DIC as the vertical displacement of the point of midspan deflection subtracted by the average vertical displacement between the support left and support right points (see Fig. 4). Then, the E_{fx} was determined by linear regression of the stress-strain curve in the strain range between 0.001 and 0.003. The experimental E_{fx} for each specimen was applied to the calculation of the fracture toughness in the fatigue tests. This allows consideration to the changes of composite materials properties due to manufacturing, aging and testing conditions.

Although the EGM is able to account for the changes of the materials elastic behavior between specimens and testing conditions, it still has limitation to account for the contribution of non-linear effects due to plastic deformation and geometry. In the case of 4ENF tests, the calculation of the SERR can be significantly affected by friction [5]. To account for these non-linear effects, a method was developed based on finite element modelling (FEM) of the steel-composite specimen [10]. Simulations of the 4ENF test were carried out using the virtual crack closure technique (VCCT) to predict the SERR at different conditions of test force (P) and crack length (a). A surface curve fit was extracted from the numerical results to correlate these parameters. A quadratic relationship was stablished for P, in order to keep the same form as the EGM – Eq. (1), and a linear relationship for a showed to be accurate enough to account for the effects of geometrical non-linearities. The fitted curve from models without friction is:

$$G_{II}^{FEM} = 0.0089P^2 - 4.98 \quad 10^{-4} \quad a + 0.076 \tag{7}$$

Eq. (7) gives similar results as the EGM. To account for friction effects, a fitted curve is extracted from models with friction, as follows:

$$G_{II}^{FEM,f} = 0.0068P^2 - 5.07 \quad 10^{-4} \quad a + 0.070 \tag{8}$$

Substituting experimental data of force and crack length into Eqs. (7) and (8), the mode II SERR of the steel-composite interface fracture can be determined with consideration to the non-linear effects.

3.3. Fatigue resistance curves

The fatigue crack growth behavior of the steel-composite bonded joints is obtained from experiments, using the crack propagation rates, measured by the DIC method in Section 3.1, and the mode II SERR, calculated by the methods in Section 3.2. The fatigue resistance curves, or Paris curves, are fitted from the test data points by the power law described in Eq. (9):

$$\frac{da}{dN} = C(G_{II})^m \tag{9}$$

where the parameters C and m are the intercept and slope of the linear segment of the Paris curve (excluding the critical and the threshold region), respectively. The Paris curve relates the fracture energy to the crack growth rate (da/dN), calculated from experimental results by the secant method between crack length measurement points, as shown in Eq. (10):

$$\left(\frac{da}{dN}\right)_a = \frac{(a_{i+1} - a_i)}{(N_{i+1} - N_i)} \tag{10}$$

where N is the number of cycles and i represents the ith data point measured during the test.

4. Results and discussion

4.1. Non-linearity effects

The mode II fracture energy (G_{II}) is obtained from the method explained in the previous section at the maximum load of the cycle. Since the tests are displacement controlled, a reduction of the applied load is expected as the crack grows, and, consequently, a reduction of the crack growth rate. Results were extracted from minimum crack steps of 1 mm to minimize measurement errors. The results from initial 20 mm of crack growth were discarded to avoid the influence of crack initiation. In addition, results from a region of 30 mm length before the second load point were neglected to avoid effects of local compression on the crack growth [10]. Friction of the interface does influence the estimation of the SERR [5]. Therefore, the effect of non-linearity was evaluated using the linear elastic EGM and the non-linear FEM-based method without and with friction effects, formulated by Eqs. (1), (7) and (8), respectively.

Fig. 6 presents a comparison between the calculated G_{II}. In Fig. 6a, similar results are shown between the EGM and the frictionless numerical model. Consequently, the Paris curves overlap in Fig. 6b. This implies a negligible effect of geometrical non-linearities of the 4ENF test. When accounting for the friction effects, the SERR reduced 30 %. This is translated into an increase of 272 % of the Paris curve C-parameter, as shown in Table 2. In addition, a slight change in the slope of the Paris curve is noticed with a reduction of 2.1 % of the m-parameter. The friction effects have significant contribution to the fatigue crack growth analysis using the 4ENF test and, therefore, the FEM-based model with friction, defined by Eq. (8), is used for the calculation of the SERR hereafter.

4.2. Reference tests

A total of 5 specimens were randomly selected from different steel-composite plates manufactured in the same conditions. A series of reference tests were performed in room conditions (21 °C) and the fatigue crack growth results of each test are shown in Fig. 7. Each test provides a significant pool of data due to the relatively long length of crack growth. Specimen RT-01 revealed consistent behavior with superior fatigue resistance while specimen RT-02 presented consistent lowest performance. In contrast, the remaining specimens (RT-03, RT-04 and RT-05) showed a transitional behavior during the tests. Higher performance is observed in earlier stages of the tests, characterized by higher crack growth rates (da/dN), and generally overlapping with specimen RT-01. Then, the fatigue performance decreased in later stages of the tests to values of SERR (G_{II}) intermediate between specimens RT-01 and RT-02.

Images of the fracture surfaces of tested specimens were obtained using a 3D optical profilometer at a magnification of x40. The fracture surfaces from reference tests are displayed in Fig. 8. Specimen RT-01 presented full composite delamination within the layer of CSM adjacent to the bonded interface, which indicates good adhesion between the steel-composite interface. On the other hand, specimen RT-02 showed full adhesive failure, which indicates poor adhesion quality of the interface between the steel and composite. Specimen RT-03 and RT-05 presented a combination of composite delamination in earlier stages and adhesive failure in later stages of crack growth. Moreover, specimen RT-04 presented dominant adhesive failure with some small chunks of fibers attached to the steel surface.

The failure modes presented in Fig. 8 can be directly corelated to the mechanical behavior observed in Fig. 7. The upper and lower bounds of the fatigue resistance of specimens RT-01 and RT-02 are related to the delamination and adhesive failure, respectively. The remaining specimens revealed combinations of these two failure modes, characterized by a crack growth from regions with more composite delamination to regions of dominant adhesive failure. These results agree with the decrease in fatigue performance during the tests in specimens RT-03, RT-04 and RT-05. Overall, the failure modes are consistent with the fatigue performance.

4.3. Effect of temperature

The effect of temperature was accessed by series of 5 tests performed in low temperature, or −10 °C, and high temperature, or 70 °C. Fig. 9 shows the Paris curves of the tests in low temperature. Representative fracture surfaces of the specimens tested in low temperature are displayed in Fig. 10. Although the fatigue behavior presented remarkable

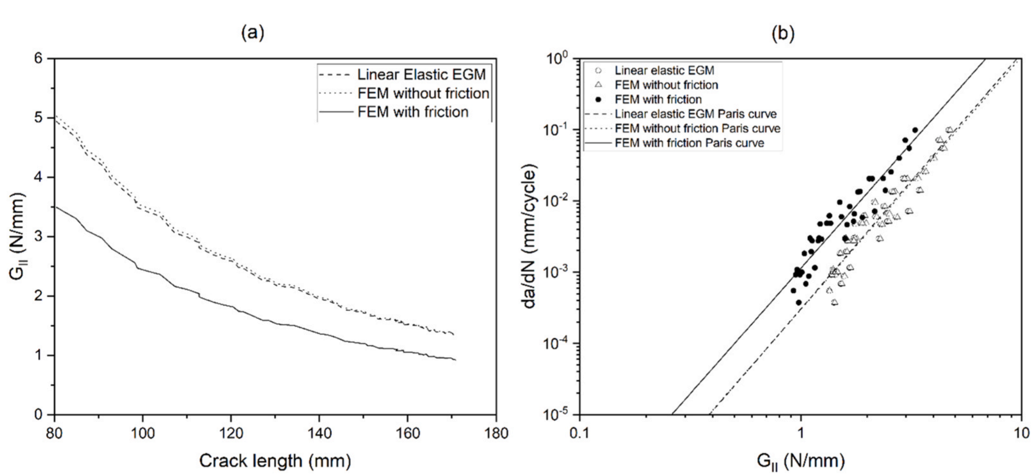

Fig. 6. Non-linearity effects on the mode II fatigue Paris curves.

Table 2
Non-linearity effects on the Paris curve parameters.

Paris curve	Linear elastic EGM	FEM without friction	FEM with friction	Effect of non-linearities
C-parameter	3.04E−4	3.00E−4	11.3E−4	272 %
m-parameter	3.59	3.55	3.51	−2.1 %

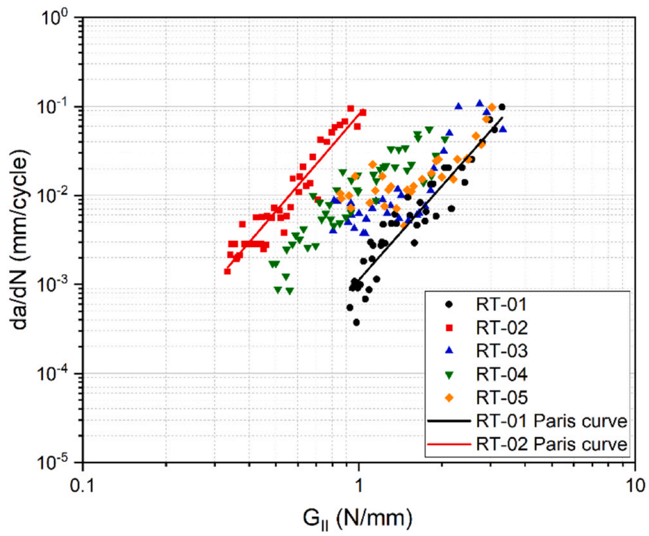

Fig. 7. Paris curves from the steel-composite interface 4ENF fatigue tests at room temperature (21 °C).

differences between tested specimens, the fracture surfaces of all specimens showed similar adhesive failure mode within the composite-steel interface.

Results of specimens tested in high temperature are presented in Fig. 11, and the representative fracture surfaces are displayed in Fig. 12. The specimens showed either a combination of composite delamination and interface failure (HT-01), or pure composite delamination (HT-03). This reveals a good adhesion quality of the composite-steel interface in high temperature. A comparison of fracture surfaces from series of tests in different temperatures reveals that low temperature tests triggered a failure of the interface while high temperature tests maintained a ductile crack growth behavior.

A summary of the Paris curve parameters (*C* and *m*) of the specimens tested in different temperatures are presented in Table 3. The results of RT-01 and RT-02 are presented as reference to the upper and lower bounds of the fatigue behavior at room temperature. Low temperature tests showed consistent *m*-parameter in specimens LT-02, LT-03, LT-04 and LT-05, while specimen LT-01 is a positive outlier. In the case of high temperature tests, a positive outlier is found in HT-02.

Fig. 13 shows the Paris curves of combined test results of each series of low and high temperatures compared to the reference tests (RT). Specimens that showed composite delamination, either in room or high temperature, consistently presented fatigue resistance near the upper bound behavior. This agrees with the observation that composite failure induces a more irregular crack path that requires more energy to grow the crack [5]. On the other hand, specimens tested in low temperature, with pure interfacial failure, showed better performance than specimens with similar failure mode tested in room conditions. These results are quantified in the combined Paris curve *C*- and *m*-parameters shown in Table 3. They were obtained using the combined results of the 5 tests from each series. Low temperature test series showed a similar value of the *m*-parameter as the reference tests, and an intermediate value of the *C*-parameter between the reference upper and lower bounds. In high temperature, the *m*-parameter is slightly higher than the reference upper bound and the *C*-parameter showed similar value. Overall, temperature changes within the operational conditions (between −10–70 °C) have a significant effect on the mode II fatigue performance of the composite-steel bonded joint. However, the variation remains within the range of results at room temperature. Low temperature does not jeopardize the performance of the interface further than the manufacturing quality.

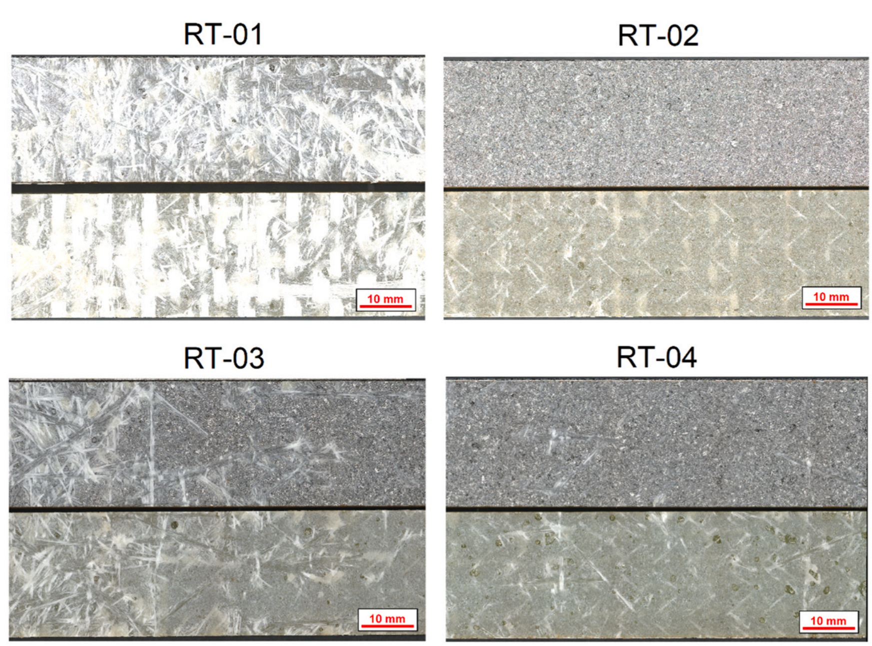

Fig. 8. Fracture surfaces from specimens tested at room temperature (crack growth direction to the right).

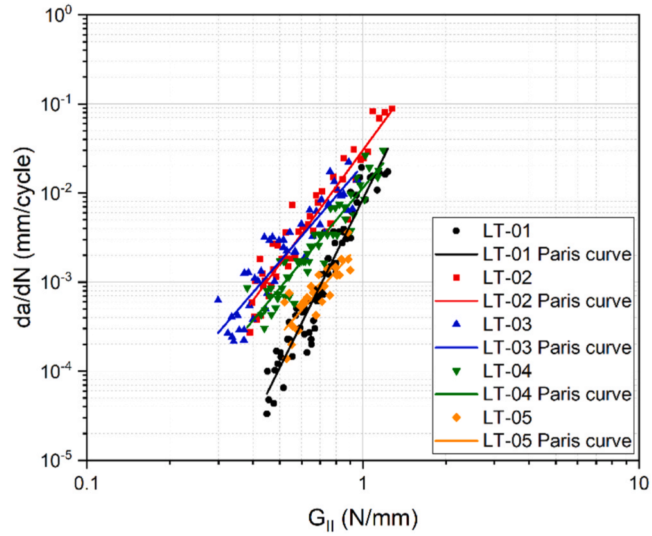

Fig. 9. Paris curves from the steel-composite interface 4ENF fatigue tests in low temperature (-10 °C).

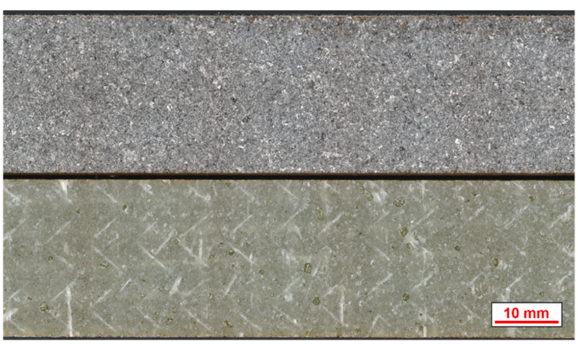

Fig. 10. Representative fracture surfaces from specimens tested at low temperature (crack growth direction to the right).

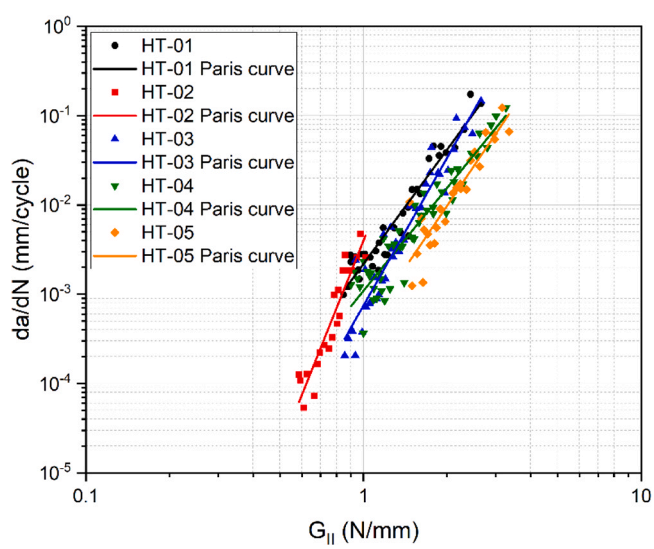

Fig. 11. Paris curves from the steel-composite interface 4ENF fatigue tests in high temperature (70 °C).

4.4. Effect of aging

The effect of aging was assessed by series of 5 tests performed after long-term immersion in saltwater. Fig. 14 shows the Paris curves of the tests in specimens aged for 222 days (RTA1). The fatigue resistance can be related to the representative fracture surfaces shown in Fig. 15. The dominant adhesive failure, observed by the bare steel surface, reveals a poor interface adhesion as consequence of the aging process. In addition, it is possible to observe an irregular pattern of corrosion on the sides of the of the steel surface. In contrast, the presence of composite delamination, observed by scattered regions of fibers attached to the steel surface, means remaining spots of good interface adhesion. Paris curves of specimens tested after 549 days of aging (RTA2) are shown in Fig. 16 and the representative fracture surface in Fig. 17. Similarly to RTA1, the failure modes are dominant adhesive within the composite-steel interface with scatter regions of composite delamination. A larger area of corrosion in noticed on the sides of the of the steel fracture surfaces compared to RTA1 (Fig. 15).

Fig. 18 shows the Paris curves of the combined test results of each series of aged specimens compared to the reference tests (RT). A significant reduction in fatigue resistance is observed between the upper bound of the reference tests and the first series of aged tests (RTA1). The second series of aged tests (RTA2), shows a slight reduction from RTA1. A summary of the Paris curve parameters (C and m) of tested aged specimens is presented in Table 4. For the reference tests, only the results of upper bound (RT-01) and lower bound (RT-02) are presented. Paris curve C- and m-parameters were also obtained using the combined results of the 5 tests from each series. There is a trend of simultaneously decreasing m-parameter and increasing the C-parameter with aging time. Overall, immersion in salt water for up to 549 days had a significant effect on the mode II fatigue performance of the composite-steel bonded joint. However, the total aging period did not reduce the fatigue performance of the interface below the lower bound of the reference non-aged tests at room temperature.

4.5. Summary

A total of 5 different testing series were carried out to evaluate the effects of short-term changes of temperature and long-term aging on the mode II fatigue behavior of composite-steel bonded joints. In addition to the reference conditions, tests were performed in low and high temperatures, and after 222 and 549 days of immersion in salt water. A reliable methodology was employed to determine the fatigue resistance from experiments. Accurate crack length measurements were extracted using DIC during the tests, and the influence of geometrical nonlinearities and friction during 4ENF tests were taken into account in the calculation of the SERR.

Lower temperatures and longer aging periods showed to degrade the joint performance. These trends are observed by the decrease in m-parameter and the increase of C-parameter of the Paris curves. The reduction of fatigue resistance reflects a transition of failure modes, from a better performance of composite delamination towards a worse performance of adhesive failure within the composite-steel interface. The correlation between mode II fatigue performance and failure mode is confirmed by the reference tests performed in non-aged specimens at room conditions. Inherent variations in the hand lay-up manufacturing process produced a range of results that variated according to the interface adhesion quality from a superior fatigue behavior, with full composite delamination, to the lowest performance, with full adhesive failure. Intermediate cases exhibited a transition between these failure modes, further emphasizing the correlation between fatigue performance and adhesion quality. Therefore, the environmental effects remained within predictable limits.

The effect of short-term changes of temperature causes physical properties of the polymer resin that may affect the interface performance. Higher temperatures typically improve the fracture toughness of

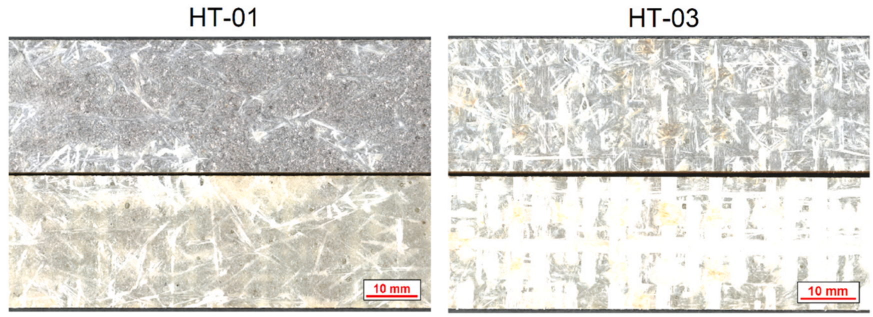

Fig. 12. Representative fracture surfaces from specimens tested at high (crack growth direction to the right).

Table 3
Paris curve parameters of low and high temperature tests.

Series	Specimen	Paris curve parameters	
		C	*m*
Reference (room temperature)	RT−01	0.00113	3.51
	RT−02	0.08160	3.62
Low temperature (−10 °C)	LT−01	0.00852	6.28
	LT−02	0.03022	4.24
	LT−03	0.02057	3.59
	LT−04	0.01141	3.74
	LT−05	0.00292	3.51
	Combined LT	0.00857	3.54
High temperature (70 °C)	HT−01	0.00219	4.24
	HT−02	0.00399	7.79
	HT−03	0.00075	5.49
	HT−04	0.00109	3.83
	HT−05	0.00040	4.60
	Combined HT	0.00127	3.89

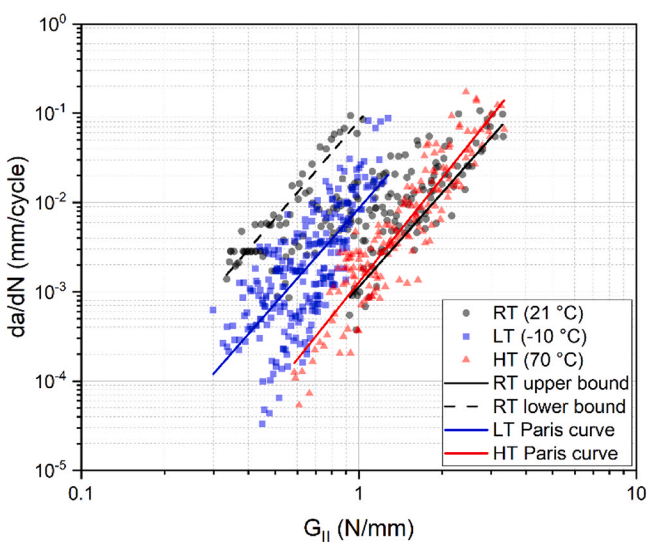

Fig. 13. Effect of temperature on the mode II fatigue Paris curves.

composites due to a larger ductility of the matrix. In contrast, lower temperatures cause embrittlement that induces more stress concentration at the bonded interface. Predictions of the temperature effects are valid within the tested range of operational temperatures (between −10 °C and 70 °C), which remains significantly below the T_g of 111 °C for the composite material [13]. Regarding the effect of long-term aging, corrosion of the steel part was observed near the edges of the interface and may contribute to further degrade the bonded joint after longer aging periods. Results highlight the importance of considering the environmental effects in design predictions of multi-material structures.

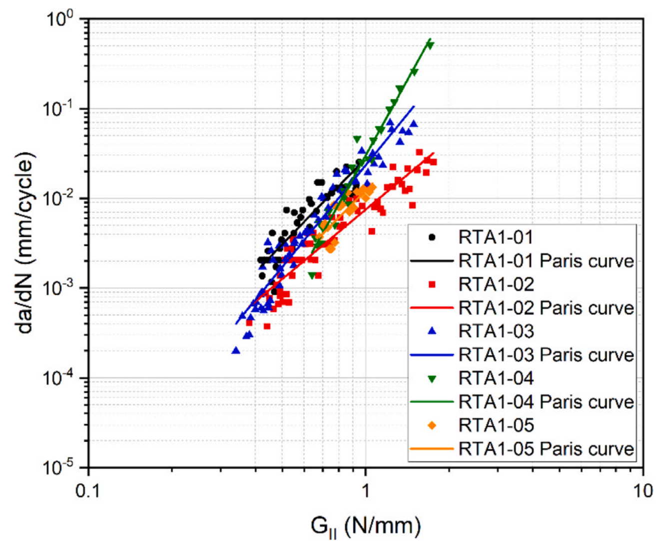

Fig. 14. Paris curves from the steel-composite interface 4ENF fatigue tests after 222 days of aging.

Fig. 15. Representative fracture surfaces from specimens tested after 222 days of aging (crack growth direction to the right).

5. Conclusion

This work investigated the effects of temperature and saltwater aging on the mode II fatigue crack growth behavior of the composite-steel bonded joint. Coupon specimens were manufactured such as the intended application of wrapped composite joints and tested using displacement controlled 4ENF tests. The consistency of the manufacturing process was evaluated by tests performed in room conditions (21 °C). Then, the range of operations temperatures was considered by tests performed in low temperature (-10 °C) and high temperature (70 °C). The effect of aging was investigated after long-term immersion in

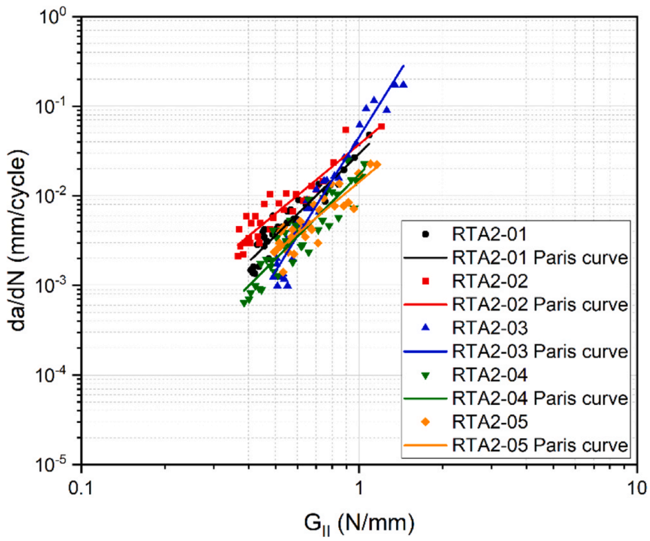

Fig. 16. Paris curves from the steel-composite interface 4ENF fatigue tests after 549 days of aging.

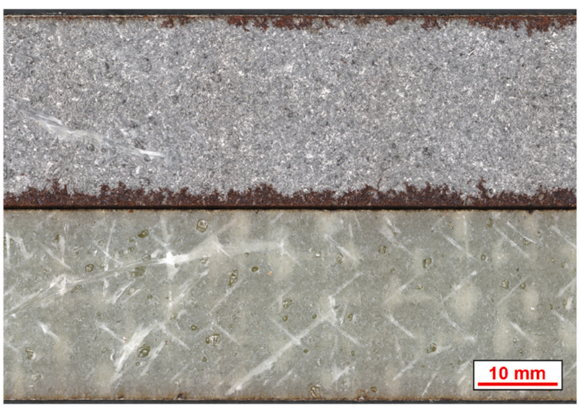

Fig. 17. Representative fracture surfaces from specimens tested after 549 days of aging (crack growth direction to the right).

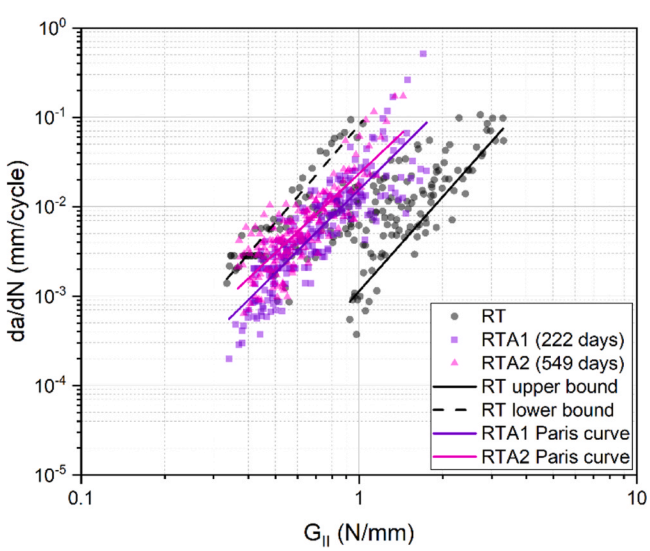

Fig. 18. Effect of aging on the mode II fatigue Paris curves.

saltwater. The following conclusions were obtained from the experimental analysis:

Table 4
Paris curve parameters of tests in aged specimens.

Series	Specimen	Paris curve parameters	
		C	*m*
Reference (non-aged)	RT−01	0.00113	3.51
	RT−02	0.08160	3.62
Aged 222 days	RTA1–01	0.02794	3.19
	RTA1–02	0.00751	2.58
	RTA1–03	0.02342	3.77
	RTA1–04	0.03010	5.59
	RTA1–05	0.01229	3.13
	Combined RTA1	0.01541	3.09
Aged 549 days	RTA2–01	0.02951	3.04
	RTA2–02	0.03757	2.57
	RTA2–03	0.04544	4.98
	RTA2–04	0.01735	3.13
	RTA2–05	0.01430	2.59
	Combined RTA2	0.02337	2.94

- Analytical methods based on LEFM are not appropriate for calculation of the SERR of 4ENF tests using composites-steel bonded joints. Friction has a significant contribution of 30 % of the energy released and must be considered in the fracture mechanics analysis. Therefore, the FEM-based methods are recommended to account for non-linear effects caused by materials and geometry;
- A relation between fatigue resistance and failure modes can be established from the experimental analysis of the mode II fatigue crack growth of composite-steel bonded joints. Higher performance is related to composite delamination, while lower performance is characterized by an adhesive failure at the bi-material interface. This can be easily observed by the presence (or not) of fibers attached to the fracture surface of the steel member.
- Reference tests produced a range of Paris curves between an upper performance, with dominant composite delamination, and a lower performance, characterized by adhesive failure within the interface. The difference in crack growth rate by a factor of 100 was found for the two boundary performances, when linear regions of the fatigue crack growth are considered;
- Temperature changes within the operational conditions (between −10 and 70 °C) have a significant effect on the mode II fatigue performance of the composite-steel bonded joint. This is followed by a clear distinction in the failure mode, with full adhesive failure in low temperature and dominant composite delamination in high temperature;
- Long-term immersion in salt water showed to reduce the mode II fatigue performance of the composite-steel bonded joint. This effect can be quantified by a simultaneous decrease of the *m*-parameter and increase of the *C*-parameter of the Paris curves with aging time;
- Neither the changes of temperature nor the aging in salt water resulted in a reduction of fatigue performance more critical than the lower bound performance found for reference tests in non-aged specimens at room temperature.

The experimental results of specimens in a range of operational temperatures and environmental aging can be used for design purposes, assuming that the resistance of the structure is governed by the resistance of the composite-steel bonded interface.

CRediT authorship contribution statement

Marko Pavlovic: Writing – review & editing, Supervision, Funding acquisition, Conceptualization. **Mathieu Koetsier:** Writing – review & editing, Investigation. **Sigurdur Egilsson:** Data curation. **Marcio Moreira Arouche:** Writing – original draft, Visualization, Validation, Methodology, Investigation, Formal analysis, Data curation, Conceptualization.

Declaration of Competing Interest

The authors declare the following financial interests/personal relationships which may be considered as potential competing interests: Marko Pavlovic reports financial support was provided by Netherlands Enterprise Agency. If there are other authors, they declare that they have no known competing financial interests or personal relationships that could have appeared to influence the work reported in this paper.

Acknowledgments

The authors would like to express their gratitude to RVO for the financial support with Topsector Energie subsidie van het Ministerie van Economische Zaken through WrapNode-I and WrapNode-II projects, and Tree Composites B.V. for the production of specimens.

References

[1] M. Heshmati, R. Haghani, M. Al-Emrani, Durability of bonded FRP-to-steel joints: effects of moisture, de-icing salt solution, temperature and FRP type, Compos. Part B Eng. 119 (2017) 153–167.
[2] M. Moreira Arouche, S. Teixeira de Freitas, S. de Barros, On the influence of glass fiber mat on the mixed-mode fracture of composite-to-metal bonded joints, Compos. Struct. 256 (2021) 113109.
[3] M.A.G. Silva, H. Biscaia, P. Ribeiro, On factors affecting CFRP-steel bonded joints, Constr. Build. Mater. 226 (2019) 360–375.
[4] M.M. Arouche, S. Teixeira de Freitas, S. de Barros, Evaluation of the strain-based partitioning method for mixed-mode I+II fracture of bi-material cracks, J. Adhes. 98 (6) (2022) 577–605.
[5] W. Feng, M.M. Arouche, M. Pavlovic, Influence of surface roughness on the mode II fracture toughness and fatigue resistance of bonded composite-to-steel joints, Constr. Build. Mater. 411 (2024) 134358.
[6] P. He, et al., Mode I fracture behavior of glass fiber composite-steel bonded interface – experiments and CZM, Compos. Struct. 330 (2024) 117814.
[7] ASTM D7905/D7905M: Standard Test Method for Determination of the Mode II Interlaminar Fracture Toughness of Unidirectional Fiber-Reinforced Polymer Matrix Composites. 2019, ASTM International.
[8] Z. Jiang, et al., Mode-II fracture behavior evaluation for adhesively bonded pultruded GFRP/steel joint using four-point bending test, Thin Walled Struct. 167 (2021) 108130.
[9] J.A. Pascoe, R.C. Alderliesten, R. Benedictus, Methods for the prediction of fatigue delamination growth in composites and adhesive bonds – a critical review, Eng. Fract. Mech. 112-113 (2013) 72–96.
[10] W. Feng, M.M. Arouche, M. Pavlovic, Fatigue crack growth characterization of composite-to-steel bonded interface using ENF and 4ENF tests, Compos. Struct. 334 (2024) 117963.
[11] S. Abdel-Monsef, et al., Effect of environment conditioning on mode II fracture behaviour of adhesively bonded joints, Theor. Appl. Fract. Mech. 112 (2021) 102912.
[12] J.J.M. Machado, et al., Mode II fracture toughness of CFRP as a function of temperature and strain rate, Compos. Part B Eng. 114 (2017) 311–318.
[13] M.M. Arouche, M. Pavlovic, Experimental and numerical analysis of the effect of temperature on the mode I and mode II delamination of glass fiber woven composites, Compos. Part B Eng. 293 (2025) 112131.
[14] J. He, G. Xian, Y.X. Zhang, Effect of moderately elevated temperatures on bond behaviour of CFRP-to-steel bonded joints using different adhesives, Constr. Build. Mater. 241 (2020) 118057.
[15] L. Ke, et al., Effects of elevated temperatures on mechanical behavior of epoxy adhesives and CFRP-steel hybrid joints, Compos. Struct. 235 (2020) 111789.
[16] D. Guo, et al., Bond behavior of CFRP-to-steel bonded joints at different service temperatures: experimental study and FE modeling, Constr. Build. Mater. 362 (2023) 129836.
[17] F.M.G. Ramírez, et al., A review on the environmental degradation effects on fatigue behaviour of adhesively bonded joints, Fatigue Fract. Eng. Mater. Struct. 43 (7) (2020) 1307–1326.
[18] D. Borrie, et al., Bond durability of fatigued CFRP-steel double-lap joints pre-exposed to marine environment, Compos. Struct. 131 (2015) 799–809.
[19] S. Teixeira de Freitas, et al., Interface adhesion assessment of composite-to-metal bonded joints under salt spray conditions using peel tests, Compos. Struct. 164 (2017) 68–75.
[20] M.M. Arouche, et al., Interlaminar adhesion assessment of carbon-epoxy laminates under salt water ageing using peel tests, Proc. Inst. Mech. Eng. Part L J. Mater. Des. Appl. 233 (8) (2018) 1555–1563.
[21] M.M. Arouche, et al., Effect of salt spray ageing on the fracture of composite-to-metal bonded joints, Int. J. Adhes. Adhes. 108 (2021) 102885.
[22] W. Feng, M. Pavlovic, Fatigue behaviour of non-welded wrapped composite joints for steel hollow sections in axial load experiments, Eng. Struct. 249 (2021) 113369.
[23] M.M. Arouche, et al., Effect of salt water ageing on the degradation of steel-composite bonded interfaces, ce/papers 6 (3-4) (2023) 293–296.
[24] D7264/D7264M - Standard Test Method for Flexural Properties of Polymer Matrix Composite Materials. 2021, ASTM International.